

## Infrared spectra of hydrogen bound to group-III acceptors in Si: Homogeneous line broadening and sidebands

M. Suezawa, N. Fukata, and M. Saito\*

*Institute for Materials Research, Tohoku University, Sendai 980-8577, Japan*

H. Yamada-Kaneta

*Fujitsu Laboratories Limited, 10-1 Morinosato-Wakamiya, Atsugi 243-0197, Japan*

(Received 18 June 2001; revised manuscript received 9 October 2001; published 1 February 2002)

We report spectral features of localized vibration of hydrogen bound to group-III acceptors in Si. To avoid the Fano effect on the line broadening, we homogeneously doped specimens with group-III acceptors and hydrogen with low concentrations; consequently, the line shapes were well fitted by Lorentzian functions, indicating that the shapes were affected by two dynamical effects, i.e., energy relaxation and dephasing. While the spectra of B-H, Al-H and Ga-H pairs were found to show only one sideband in the lower-frequency region of the main peak, sidebands appeared in both the lower- and higher-frequency regions in the case of In-H. This appearance of the sidebands in the case of In-H pairs was unexpected from a previous model [M. Stavola *et al.*, Phys. Rev. B **37**, 8313 (1988)]. By analyzing the linewidth of the main peak at around 6 K, we estimated the energy relaxation times  $T_1$ , which were found to be much shorter than those previously observed for the complexes of the point defect and H in Si. Moreover, we also found a chemical trend: As the covalent radius of the group-III acceptor increased, the  $T_1$  became shorter. Temperature dependences of the linewidth and peak shift of the main peak were analyzed based on dephasing models. The analysis showed that the experimental results cannot be explained by the Persson-Ryberg model in the weak-coupling limit of the anharmonic coupling between the local vibrational mode and bath ones, suggesting that the anharmonic coupling is intermediate or strong.

DOI: 10.1103/PhysRevB.65.075214

PACS number(s): 78.30.Am, 63.20.Pw, 63.20.Kr

### I. INTRODUCTION

Since the pioneering study of Pankove *et al.*<sup>1</sup> on the hydrogen (H) passivation of B in Si by the formation of B-H pairs, various experimental techniques have been used to study the properties of H itself and H-related complexes in Si.<sup>2-4</sup> Among a variety of methods, optical absorption spectroscopy of LVM (localized vibrational mode) due to H is a useful tool for determining their properties since the frequency of LVM is sensitive to the configuration around H. It is much higher than the bulk phonon frequency and its detectability is high. Such LVM sometimes displays peculiar behaviors. As for pairs of group-III acceptors and H (abbreviated as III-H pairs hereafter) in Si, there are at least two interesting features. One is the appearance of a peak at high temperatures and the other is strong temperature dependences of the linewidth and peak position of LVM.

As for the first feature, Stavola *et al.*<sup>5,6</sup> first reported not only optical absorption peaks (the main peaks) observed at around 5 K, but also side peaks at lower energy of the main peaks at high temperatures. They interpreted the appearance of a side peak to be due to anharmonic coupling between the H vibration of the main peak and a low-frequency mode, which is presumably characterized by the wagging motion of H. They doped Si with group-III acceptors by an ion-implantation method and passivated them by hydrogen-plasma treatment. The line shapes were asymmetric except for those of Al-H pairs because of the Fano effect, which is due to the interaction between the vibrational state and free carriers of high density. Hence, they succeeded in analyzing the data of Al-H only.

As for the second feature, the linewidth is known to be determined by two dynamical processes, i.e., energy relaxation (relaxation time  $T_1$ ) and pure dephasing ( $T_2$ ).<sup>7</sup> Budde *et al.*<sup>8</sup> showed that the spectral line shape of bond-centered hydrogen is determined by  $T_1$  at a low temperature, 10 K. For the complexes of the point defect and hydrogen where the hydrogen is bound to one Si atom, which is bonded with three Si atoms [(Si)<sub>3</sub>-Si-H], Budde *et al.*<sup>8</sup> found that the  $T_1$  deduced from the observed linewidth were similar to each other. To clarify the dephasing mechanism, we previously analyzed<sup>9</sup> the observed spectra of the above complexes and found that the temperature dependence of the linewidth and that of the peak shift are well explained in terms of the Persson-Ryberg model<sup>10</sup> in the weak-coupling limit of the anharmonic coupling. In the case of III-H pairs, the hydrogen is located between one Si host atom and a group-III atom [H at bond-centered (BC) site], so the local geometry around the hydrogen is quite different from those of [(Si)<sub>3</sub>-Si-H] systems. Although it is thus of interest to study  $T_1$  and  $T_2$  of the III-H systems, such study has not yet been performed. To do this, we need to observe the symmetrical line shape.

In this study, we examined both features of III-H pairs and herein report systematic results. To obtain a symmetrical line shape allowing full analysis of the optical absorption spectra, we should avoid the Fano effect. For this purpose, it is necessary to study specimens doped with group-III acceptors with a much lower concentration than that in the study of Stavola *et al.* In such case, since the specimen size should be sufficiently large to observe optical absorption peaks, it is necessary to introduce H homogeneously throughout bulk specimens with a method other than hydrogen-plasma treat-

ment, which passivates acceptors near the surface regions only. We adopted a high-temperature treatment method for homogeneous H doping, namely, annealing specimens in  $H_2$  gas at high temperature followed by quenching.<sup>11,12</sup> By using this method for H doping of Si crystal homogeneously pre-doped with acceptors during crystal growth, we obtained symmetrical optical absorption peaks due to III-H pairs and analyzed their line shapes with Lorentzians. The symmetrical line shapes of the main peak and side peak also made it possible to analyze the temperature dependences of the linewidth and peak position as well as their intensities.

The main conclusions deduced from our experiments are as follows.

(1) Besides B-H, Al-H and Ga-H pairs, we examined an In-H pair with unexpected results: While the other pairs showed only one side peak in the low-frequency regions as Stavola *et al.*<sup>5,6</sup> reported, the In-H pair showed several side peaks in both the low- and high-frequency regions, implying that the model by Stavola *et al.* is inadequate at least for this pair.

(2) We deduced the relaxation times  $T_1$  from the spectra at 6 K and found them to be much shorter than those of H-point defect complexes.

(3) The Persson-Ryberg dephasing model<sup>10</sup> in the weak-coupling limit was found not to explain the temperature dependence of the linewidth and peak shift of the main peaks, suggesting that the anharmonic coupling is intermediate or strong. This result is in sharp contrast with those of  $[(Si)_3-Si-H]$  systems whose spectra are well explained by the weak-coupling model.

We briefly explain the experimental procedure in Sec. II. In Sec. III, we show experimental results, such as the formation of III-H pairs and optical absorption spectra of various III-H pairs. Analysis and discussion of the experimental results are presented in Sec. IV.

## II. EXPERIMENTAL

Specimens were grown by a floating-zone growth method. These specimens were doped with group-III elements such as B, Al, Ga, and In during crystal growth at concentrations of  $3 \times 10^{15}$ ,  $2 \times 10^{15}$ ,  $5 \times 10^{15}$ , and  $3 \times 10^{15} \text{ cm}^{-3}$ , respectively. Specimens were cut out from the above crystals with a diamond slicer. After cutting, they were mechanically shaped with carborundum and chemically etched with an etchant of mixed acid,  $HNO_3:HF=5:1$ . Specimen size was about  $6 \times 6 \times 11 \text{ mm}^3$ . For doping the specimens with H, they were sealed in quartz capsules together with  $H_2$  gas and heated at  $1300^\circ\text{C}$  for 1 h followed by quenching in water. Most hydrogen atoms are in a molecular state,  $H_2$ .<sup>13</sup> We annealed the specimens at  $150^\circ\text{C}$  to form III-H pairs.<sup>11,12</sup> We measured their optical absorption spectra by a Fourier transform infrared spectrometer equipped with a temperature-variable cryostat. The resolution was  $0.5 \text{ cm}^{-1}$  and the measurement temperature range was between 6 K and RT.

## III. EXPERIMENTAL RESULTS

### A. Formation of acceptor-H pairs due to isochronal annealing

After hydrogenation, we annealed specimens at  $150^\circ\text{C}$  to form III-H pairs.<sup>11,12</sup> Figure 1 shows the formation of III-H

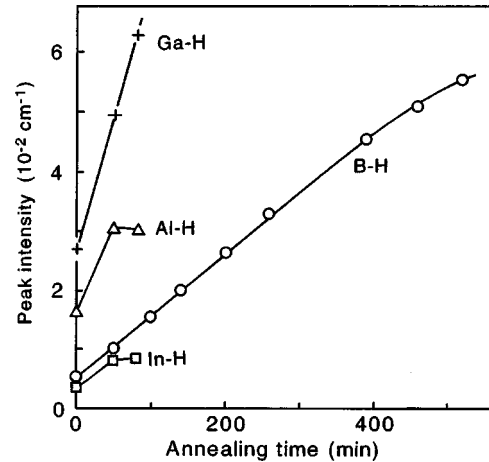


FIG. 1. Generation of group III acceptor-H pairs due to isothermal annealing at  $150^\circ\text{C}$ . The ordinate is the peak intensity.

pairs due to isothermal annealing. Immediately after hydrogenation, only a part of the acceptors formed pairs with H. This is probably due to the high quenching rate after H doping and, consequently, insufficient time for diffusion of H atoms to form III-H pairs. The formation process at  $150^\circ\text{C}$  was dominated by the diffusion of  $H_2$  (Ref. 14) to acceptor atoms since acceptor atoms are immobile at this temperature and H exists as a state of  $H_2$  (Ref. 13) after hydrogenation with the above method. Actually, an optical absorption peak was observed at  $3618 \text{ cm}^{-1}$  due to the vibration of  $H_2$ .<sup>13</sup> The formation process of the above pairs is discussed in Sec. IV.

### B. Spectra and their temperature dependence

Figures 2–5 show the optical absorption spectra of B-H, Al-H, Ga-H, and In-H pairs, respectively, at various tempera-

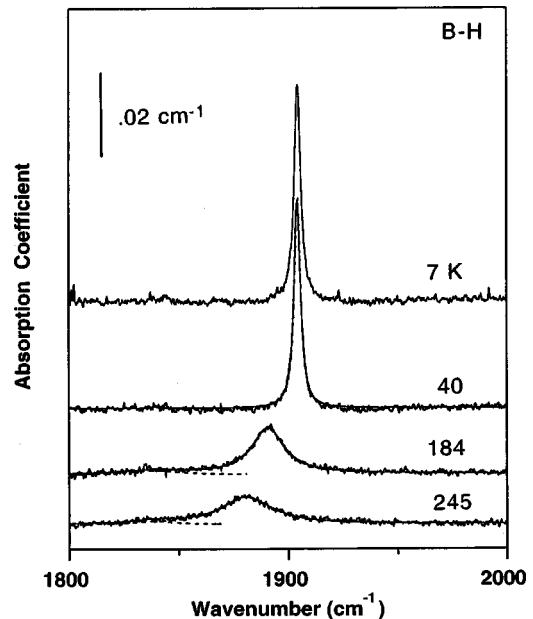


FIG. 2. Optical absorption spectra due to the B-H pair at various temperatures. Smooth solid and dashed lines are sums and decomposed fitting curves by Lorentzians, respectively.

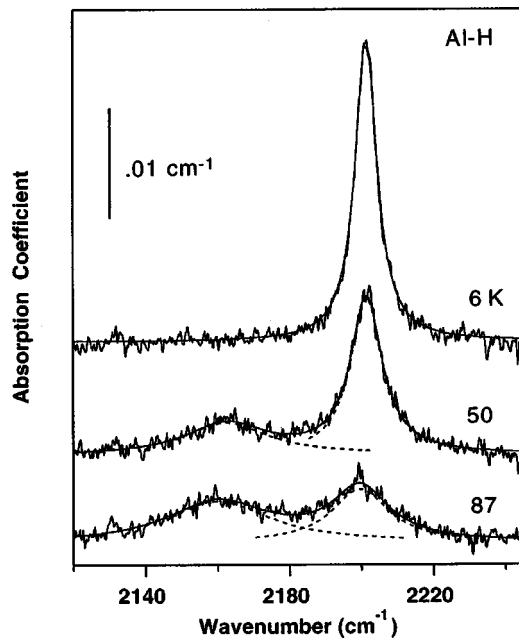


FIG. 3. Optical absorption spectra due to the Al-H pair at various temperatures. Smooth solid and dashed lines are sums and decomposed fitting curves by Lorentzians, respectively.

tures. The spectra of B-H, Al-H, and Ga-H pairs were similar to those of Stavola *et al.*<sup>5,6</sup> except for the symmetrical line shape in our case, which was an expected result. Dashed lines and smooth solid lines represent decomposed peaks with Lorentzian functions and their sums, respectively. In the case of the B-H pair, there was a strong peak (the main peak) at around 7 K and a very weak peak (the side peak) at high temperatures at the lower energy side of the main peak. The

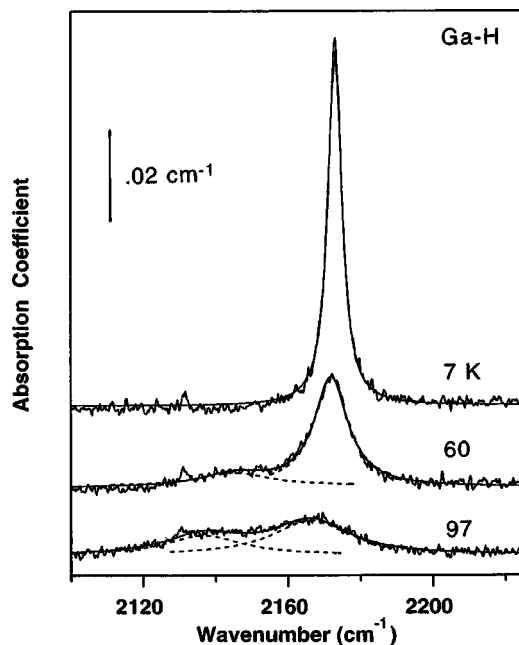


FIG. 4. Optical absorption spectra due to the Ga-H pair at various temperatures. Smooth solid and dashed lines are sums and decomposed fitting curves by Lorentzians, respectively.

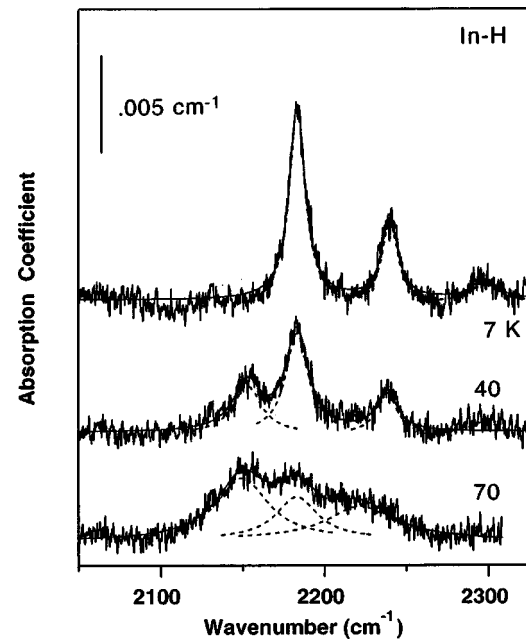


FIG. 5. Optical absorption spectra due to the In-H pair at various temperatures. Smooth solid and dashed lines are sums and decomposed fitting curves by Lorentzians, respectively.

intensity of the side peak was too weak to be analyzed and thus we will not discuss this side peak hereafter. In the cases of Al-H and Ga-H pairs, there was a strong peak (the main peak) at around 7 K and a weak peak (the side peak) at high temperatures at the lower-energy side of the main peak, which depends on the temperature. The solid lines fit well with the observed spectra. On the other hand, in the case of the In-H pair, the spectrum was much different from those of other III-H pairs, as shown in Fig. 5. There are three peaks in the spectrum at 7 K. These peaks grew due to annealing at 150 °C and, simultaneously, intensities of peaks due to electronic transitions of In decreased. Moreover, we observed two peaks at 1582.6 and about 1639  $\text{cm}^{-1}$  after annealing of a specimen doped with deuterium. The third peak (the highest-energy peak) was not observed probably due to very weak intensity. Hence, these three peaks are considered to be due to the In-H pair. The frequency ratios of corresponding peaks due to In-H and In-D pairs are different from each other, which cannot yet be explained. The peak separations between a peak and the peak on its right are almost the same, about 58.0 and 56.5  $\text{cm}^{-1}$ . We consider that the strongest peak corresponds to the main peaks of other III-H pairs. Similar to Al-H and Ga-H pairs, a weak peak appeared at the lower-energy side of the main peak. There seem to be no side peaks associated with two peaks at higher energies in the In-H pair. The magnitudes of the peak shift of the side peak from the main peak were similar for all III-H pairs, i.e., 37, 28, and 32  $\text{cm}^{-1}$  for Al-H, Ga-H, and In-H pairs, respectively.

## IV. ANALYSIS AND DISCUSSION

### A. Formation of acceptor-H pairs

We first discuss the formation process of III-H pairs. As explained already, most hydrogen atoms are in the state of

$H_2$  (Ref. 13) when doped by the method adopted in this study. To form a III-H pair, an  $H_2$  should diffuse to an acceptor atom since the former is mobile<sup>14</sup> while the latter is immobile at around 100 °C. Moreover, it should dissociate into two H atoms to form a III-H pair. Here we discuss the loss and gain of energy. According to Van de Walle,<sup>15</sup> dissociation energy is estimated to be about 1.74 eV per one  $H_2$ . According to Zundel and Weber,<sup>16</sup> on the other hand, the binding energies of B-H, Al-H, Ga-H, and In-H pairs are similar, namely, about 1.28, 1.44, 1.40, and 1.42 eV, respectively. Hence, if two H atoms form two pairs with acceptor atoms ( $2\text{III} + H_2 \rightarrow 2\text{III-H}$ ), the energy gain is between 0.82 (B-H pair) and 1.14 eV (Al-H pair). Therefore, the pair formation is favorable. At an intermediate state, i.e.,  $\text{III} + H_2 \rightarrow \text{III-H} + H$ , on the other hand, energy gains are between 0.41 (B-H pair) and 0.57 eV (Al-H pair). Hence, pair formation is favorable at any stage.

According to Fig. 1, the formation process seems to depend on the acceptor species. In the cases of Al and In, their peak intensities were saturated after annealing of short duration. Prior to this experiment, we annealed for longer times expecting higher concentrations of Al-H and In-H pairs. Their intensities, however, decreased due to annealing at longer than 100 min. Even after saturation, optical absorption due to electronic transition of isolated acceptors and that due to vibrational transition of  $H_2$  were still strong. This means that there were still many isolated entities,  $H_2$  and acceptors. Intuitively, the saturation seems to be explained by the binding energies between H and acceptor atoms because the forward and backward reactions of  $2\text{III} + H_2 \leftrightarrow 2\text{III-H}$  are dynamically balanced at the saturated state. As cited above, they have similar magnitudes. Hence, another explanation for the saturation is required since the densities of B-H and Ga-H pairs continue to increase as shown in Fig. 1.

### B. Temperature dependencies of the ratios of main peaks and side peaks

Next, we discuss the temperature dependence of the intensity ratio of the side peak and main peak. We analyzed the ratio of intensities of the main peak and the side peak in the same way as Stavola *et al.*<sup>6</sup> Referring to oxygen vibration in Si, they interpreted that the side peak was due to anharmonic coupling of the low-frequency wagging vibration of H and the higher-frequency stretching vibration of H. According to them, the main peak and the side peak correspond to the transition between the lowest states of the ground and upper states and that between the first-excited states in the ground and upper states, respectively, as shown in Fig. 6, which was slightly modified from that of Stavola *et al.*<sup>6</sup> Hence, the temperature dependence of the ratio of intensities corresponds to the energy separation between the lowest- and the first-excited state in the ground state. To determine this energy, we made the Arrhenius plot of intensity ratio, as shown in Fig. 7, which shows the results for the Al-H, Ga-H, and In-H pairs. The integrated intensities were determined from spectral decomposition by Lorentzians. By applying a function of  $\exp[-E/kT]$ , we obtained  $E$  which is the energy separation in

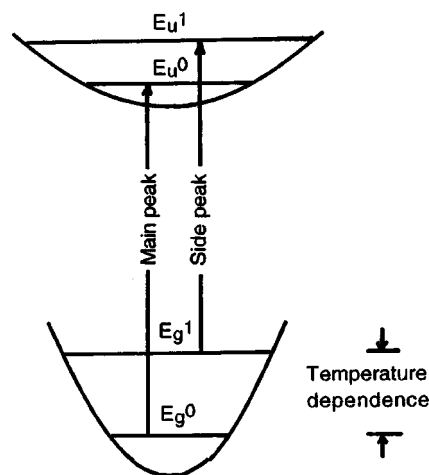


FIG. 6. Model proposed by Stavola *et al.* to explain the main peak and side peak.  $E_x^y$  corresponds to energy level at  $x$  ( $g$ : ground state,  $u$ : upper state).  $Y=0$  and  $1$  denote the lowest- and the first-excited levels, respectively.

the ground state as shown in Fig. 6. The value of the Al-H pair is about  $78 \text{ cm}^{-1}$ , which agrees well with that of Stavola *et al.*<sup>6</sup> The value of the Ga-H pair was about  $147 \text{ cm}^{-1}$ . In the case of the In-H pair, two temperature dependences were obtained, i.e.,  $183 \text{ cm}^{-1}$  at high temperatures and  $20 \text{ cm}^{-1}$  at low temperatures. The temperature dependence, except that of In-H pair at a low temperature, increases with the atomic number of the acceptor.

In the above, we analyzed the side peak located lower than the main peak. It should be noticed, however, that the side peaks located higher than the main peak in In-H pair cannot be explained by the model of Stavola *et al.* Some discussion on the side peaks is given in the following section.

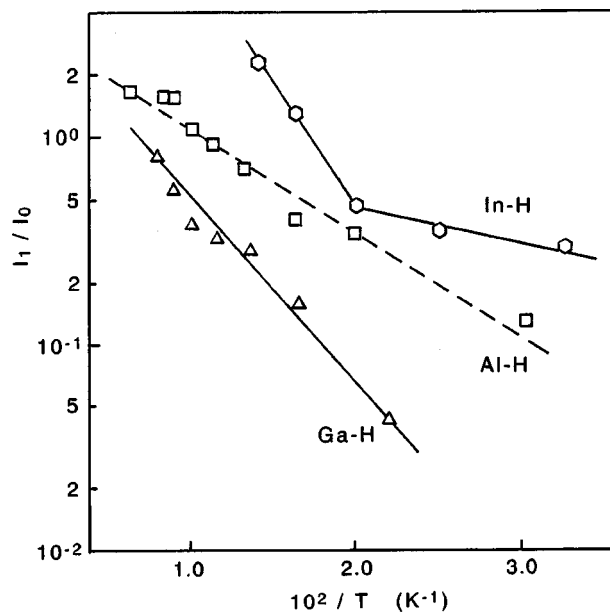


FIG. 7. Temperature dependence of the intensity ratio of the side peak and main peak. Peak intensity is the integrated intensity.

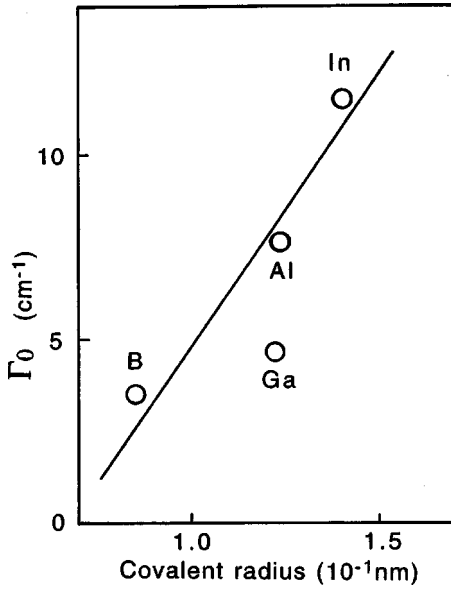


FIG. 8. Dependence of the full width at half maximum of the main peak of various III-H pairs at 6 K on the covalent radius.

### C. Relaxation time, $T_1$

We first deduce  $T_1$  from the spectra observed at about 6 K. At this very low temperature, it is expected that the dephasing process can be neglected. Thus,  $T_1$  is deduced from the linewidth ( $\Gamma_0$ ) as  $1/2c\pi\Gamma_0$ .<sup>8</sup> Indeed, by means of time-resolved, transient bleaching spectroscopy, Budde *et al.*<sup>8</sup> have shown that the vibrational lifetimes of LVM of bond-centered H in Si at low temperatures are dominated by the energy relaxation process. As shown in Fig. 8,  $\Gamma_0$  values strongly depend on the acceptor species. Moreover, they are much larger than those, typically below  $1\text{ cm}^{-1}$ , of H-point defect complexes in Si.  $\Gamma_0$  has a roughly linear dependence on the covalent radius.  $T_1$ 's estimated from the experimental  $\Gamma_0$ 's are shown in Table I together with those of H-point defect complexes and  $H_2^*$ .<sup>9</sup>

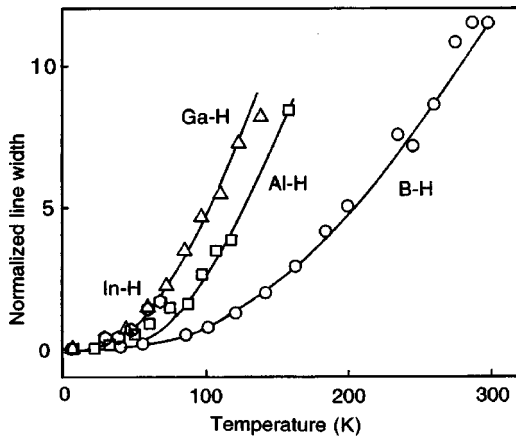


FIG. 9. Dependences of normalized linewidths of the main peak on temperature. Solid lines are fitting curves due to Eq. (1).

TABLE I. Relaxation time  $T_1$  of III-H pairs and H-point defect complexes in Si.  $I$  and  $V$  indicate a self-interstitial and a vacancy, respectively.  $VH_2$ , for example, means a complex composed of one  $V$  and two H atoms. The relation between complexes and their peak positions are as follows:  $H_2^*(AB)$ ,  $1838\text{ cm}^{-1}$ ;  $H_2^*(BC)$ ,  $2062$ ;  $I_2H_2$ ,  $1870$ ;  $IH_2(1)$ ,  $1987$ ;  $IH_2(2)$ ,  $1990$ ;  $V_2H_2$ ,  $2072$ ;  $VH_2(1)$ ,  $2122$ ;  $VH_2(2)$ ,  $2145$ .

Species	$T_1$ (ps)	Species	$T_1$ (ps)
B-H	1.5	$H_2^*(AB)$	3.1
Al-H	.70	$H_2^*(BC)$	1.8
Ga-H	1.2	$I_2H_2$	6.3
In-H	.46	$IH_2(1)$	7.3
		$IH_2(2)$	7.2
		$V_2H_2$	15
		$VH_2(1)$	17
		$VH_2(2)$	16

### D. Analysis of temperature dependencies of linewidth and peak position

We here discuss the temperature dependence of the main peak. Since the dephasing time rapidly decreases as the temperature becomes high, the linewidth is expected to be dominated by the dephasing process except at very low temperatures, where the energy-relaxation process is dominant. Thus, the dephasing time is approximately given by  $1/(\Gamma - \Gamma_0)$ . We thus introduce the normalized linewidth  $(\Gamma - \Gamma_0)/\Gamma_0$  to analyze the dephasing process. Perrson and Ryberg<sup>10</sup> considered the case wherein the LVM is coupled with bath modes having a single frequency  $\omega_0$ . In the weak-coupling limit, where the anharmonic coupling  $\delta\omega$  between the LVM and bath modes is much smaller than the energy width  $\eta$  of the bath modes, they obtained the analytic expressions of Eqs. (1) through (3).

Weak-coupling limit.  $|\delta\omega| \ll \eta$ .

$$\Delta\omega = \delta\omega/\beta, \quad (1)$$

$$\Delta\Gamma = (2\delta\omega^2/\eta)(\beta+1)/\beta^2, \quad (2)$$

$$\Delta\Gamma/(\Delta\omega)^2 = 2(\beta+1)/\eta, \quad (3)$$

where  $\beta = \exp(\hbar\omega_0/kT) - 1$ ,  $\delta\omega$  is the coupling constant of two modes,  $\omega_0$  is the vibrational frequency of the coupling low mode with linewidth  $\eta$  and  $\hbar$  = (Planck constant)/ $2\pi$ . Although it is interesting to study the strong coupling case, its analytic expressions has not been obtained.

Another model assumes that all acoustic phonons of lattice modes interact with the LVM. This model was developed by McCumber and Sturge<sup>17</sup> and applied by Elliott *et al.*<sup>18</sup> to explain the temperature dependences of the linewidth and peak position of the localized mode of H in alkaline earth fluorides. Under the assumptions of an isotropic Debye model for the acoustic phonons and no interaction with the optical phonons, they obtained the following temperature dependences:

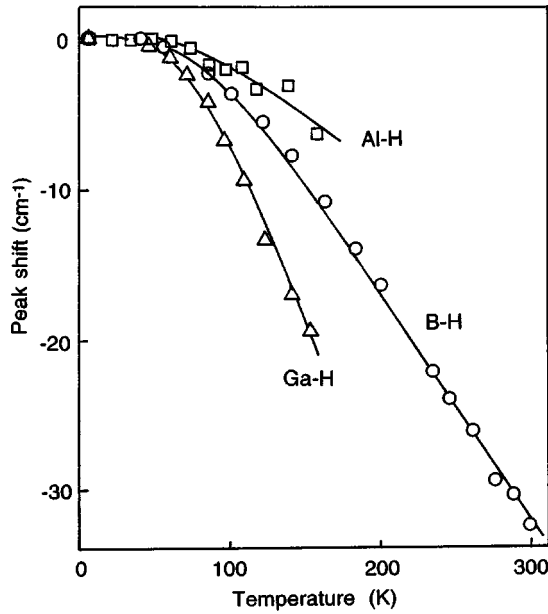


FIG. 10. Dependence of the peak shifts on temperature. Solid lines are fitting curves due to Eq. (2).

$$\Delta\omega(T) = A \left( \frac{T}{\Theta} \right)^4 \int_0^{\Theta/T} \frac{x^3}{e^x - 1} dx \quad (4)$$

$$\Delta\Gamma(T) = B \left( \frac{T}{\Theta} \right)^7 \int_0^{\Theta/T} \frac{x^6 e^x}{(e^x - 1)^2} dx \quad (5)$$

for the peak position and the linewidth, respectively. Here,  $\Delta\omega$ ,  $\Delta\Gamma$ , and  $\Theta$  are the peak shift, change of the linewidth, and the effective Debye temperature, respectively.  $T$  is the measurement temperature and  $A$  and  $B$  are constants.

First, we examine the weak coupling case. We fit Eqs. (1) through (3) to the experimental data independently (details of these fitting procedures were described previously<sup>9</sup>). Fittings were good as shown in Fig. 9 for linewidth, Fig. 10 for peak position, and Fig. 11 for fitting with Eq. (3). The obtained  $\omega_0$  for the three equations, however, are different from each other (Table II), indicating that the weak-coupling model interacting with one-phonon mode cannot explain the experimental data.

Next, we examine the dephasing model interacting with all transverse acoustic modes assuming the Debye model. We obtain  $\Theta$  in two ways, i.e., we fit Eq. (4) or Eq. (5) to the data. Each fitting, again, was good. As shown in Table III, however, the two values are different from each other in the case of Al and Ga, indicating that this model does not work. On the other hand, the two values are close to each other in the case of B, thus the fitting is successful. This agreement, however, might be accidental.

## V. DISCUSSION

As mentioned in Sec. IV C, the obtained  $T_1$  are much shorter than those of H-point defect complexes (Table I), indicating that there are efficient relaxation paths in the case of III-H pairs. Among the H-point defect complexes and hy-

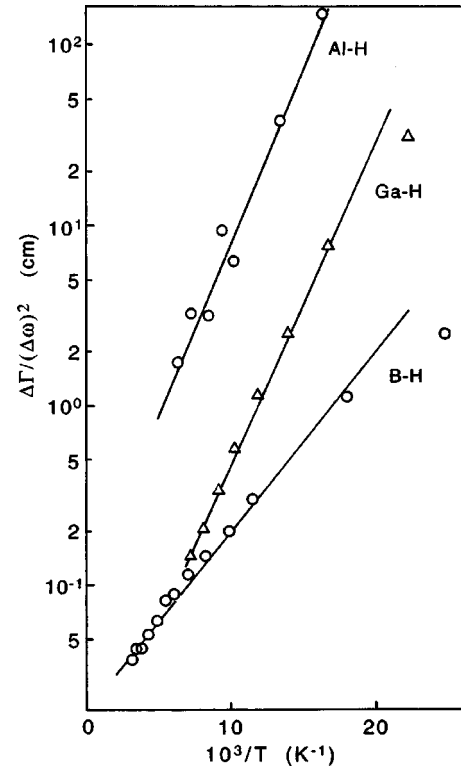


FIG. 11. Relation of  $\Delta\Gamma/(\Delta\omega)^2$  and  $1/T$  [Eq. (3)].

drogen pairs, the  $2062 \text{ cm}^{-1}$  peak in  $\text{H}_2^*$  has the shortest relaxation time, similar to that of the B-H pair. This peak is due to the motion of H located at the bond-centered site. The short relaxation time is thought to be due to the fact that the coupling of the observed mode with the surrounding lattice modes is great since this hydrogen atom is squeezed by the nearest two Si atoms. In the III-H pair, the hydrogen atom occupies the bond-centered site and is also squeezed by two atoms (one is the Si atom and the other is an acceptor atom). This is thought to be the reason why the relaxation process is efficient in the III-H pairs. The relaxation time strongly depends on the acceptor atoms, i.e., it becomes much shorter as the covalent radius increases. This is thought to be due to the fact that the squeezing becomes stronger as the covalent radius increases.

As mentioned in Sec. IV D, the Perrson-Ryberg model<sup>10</sup> in the weak-coupling limit cannot explain the temperature dependence of the main peak. We expect that this failure of the model is due to the fact that the condition  $|\delta\omega| \ll \eta$  is not satisfied. Although our fittings of Eqs. (1)–(3) were not suc-

TABLE II. Parameters determined from fittings.  $\omega_0(1)$ ,  $\omega_0(2)$ , and  $\omega_0(3)$  were determined from peak shift, linewidth, and  $\Delta\Gamma/(\Delta\omega)^2$ , respectively.

	$\delta\omega$ ( $\text{cm}^{-1}$ )	$\omega_0(1)$ ( $\text{cm}^{-1}$ )	$\omega_0(2)$ ( $\text{cm}^{-1}$ )	$\omega_0(3)$ ( $\text{cm}^{-1}$ )	$\eta$ ( $\text{cm}^{-1}$ )
B-H	-51	283	292	159	27
Al-H	-21	236	194	304	38
Ga-H	-113	282	87	287	116

TABLE III. Debye temperature  $\Theta(1)$  and  $\Theta(2)$  were determined from fitting of peak shift and linewidth, respectively.

	$\Theta(1)$ (K)	$\Theta(2)$ (K)
B-H	404	413
Al-H	403	200
Ga-H	454	104

cessful, the estimated values of  $\delta\omega$  are thought to be valid except for the case of very strong coupling. The values of  $|\delta\omega|$  are much larger than those of H-point defect complexes to which the weak-coupling model is applicable ( $10\text{--}16\text{ cm}^{-1}$ ), indicating that the strong anharmonic coupling is expected to be the reason why the weak-coupling model is not applicable. It should be noticed that the  $2062\text{ cm}^{-1}$  peak of  $\text{H}_2^*$ , where the geometrical situation is similar to those of III-H pairs, also has a somewhat large value of  $|\delta\omega|$  ( $19.8\text{ cm}^{-1}$ ) and that the weak-coupling model is not applicable. It is, therefore, speculated that the strong anharmonic coupling in the dephasing process as well as the above-mentioned short  $T_1$  are due to the local atomic structures where H is squeezed by two neighboring atoms.

It is known that in the strong-coupling case, some sidebands due to the low-frequency mode appear. Thus the side peaks observed in our experiment may be due to the strong coupling discussed above. Zhang and Langreth<sup>19</sup> concluded that the strong third anharmonic term causes side peaks both in the lower- and higher-frequency regions,  $\omega \pm \omega_0$ ,  $\omega \pm 2\omega_0, \dots$ . Although this model is still insufficient to explain the side peaks of In-H pairs, which appear in both lower and higher.

The anomalous features of the side peaks in In-H pairs might be due to the situation that H occupies the antibonding (AB) site as well as H at the BC site, assuming that the LVM frequencies in the case of the AB site are higher than that of H at the BC site. Indeed the existence of two kinds of H was proposed by Wichert *et al.*<sup>20</sup> based on their experimental results of PAC (perturbed angular correlation) and the channeling: They observed two kinds of In-H pairs with  $\langle 111 \rangle$  symmetry. Later, however, Wichert *et al.*<sup>21</sup> showed that H at BC and AB sites are dominant at low and high temperatures, respectively, and that the population of H at AB is negligibly small at 10 K. Hence, the idea of two kinds of H in In-H pairs cannot explain our finding of side peaks since those peaks were observed even at low temperatures such as 6 K.

## VI. CONCLUSION

We studied infrared spectra of III-H pairs in Si. In order to obtain the Lorentzian line shapes, which provide information on the two dynamical processes characterized by  $T_1$  and  $T_2$ , we homogeneously doped specimens with low concentrations of hydrogen and group-III acceptors. While the spectra of B-H, Al-H, and Ga-H pairs show only one side peak in the lower-frequency region of the main peak, side peaks appear in both the lower- and higher-frequency regions in the spectra of In-H. These side peaks are unexplained by a previous model proposed by Stavola *et al.*

We estimated the energy-relaxation times  $T_1$  from the spectra observed at low temperature, 6 K, and found their values to be much shorter than those of the complexes of the point defect and hydrogen. We also found that there is a chemical trend: as the core radius of the group-III atoms increases,  $T_1$  becomes shorter. Furthermore, it was found that the temperature dependence of the linewidth and line shift of the main peak were not explained by the Persson-Ryberg dephasing model in the weak-coupling limit, suggesting that the anharmonic coupling is intermediate or strong.

Our findings on the sidebands, short  $T_1$ , and anharmonic coupling, which is not small in the dephasing process, are quite different from those in the hydrogen point-defect complexes whose local structures are  $[(\text{Si})_3\text{-Si-H}]$ . It is expected that the difference originates from the fact that the local atomic structures are different as discussed in Sec. V: In III-H pairs, the hydrogen atoms are squeezed by one Si and one impurity (III) atoms, while the Si-H bond rather freely vibrates in the  $[(\text{Si})_3\text{-Si-H}]$  geometry. A theory that takes this local structure of the III-H pairs into consideration is expected to explain our findings in the observed spectra.

## ACKNOWLEDGMENTS

The authors wish to thank the Laboratory for Developmental Research of Advanced Materials for allowing them to use its facilities to measure the optical absorption of specimens. This work was partly supported by JSPS Research for the Future Program under the Project ‘‘Ultimate Characterization Technique of SOI Wafers for Nano-scale LSI Devices’’ and a Grant-in-Aid for Scientific Research on Priority Areas (B), ‘‘Manipulation of Atoms and Molecules by Electronic Excitation,’’ by the Japanese Ministry of Education, Culture, Sports, Science and Technology.

\*Permanent address: NEC Informatel Systems Ltd., 34 Miyuki-gaoka, Tsukuba 305-8501, Japan.

<sup>1</sup>J. I. Pankove, D. E. Carlson, J. E. Berkeyheiser, and R. O. Wance, Phys. Rev. Lett. **51**, 2224 (1983).

<sup>2</sup>As a review article, *Hydrogen in Semiconductors I*, edited by J. I. Pankove (Academic, New York, 1990).

<sup>3</sup>As a review article, S. J. Pearton, J. W. Corbett, and M. Stavola, *Hydrogen in Crystalline Semiconductors* (Springer-Verlag, Berlin, 1992).

<sup>4</sup>As a review article, M. D. McCluskey and E. E. Haller, *Hydrogen in Semiconductors II*, edited by N. H. Nickel (Academic, New York, 1999), p. 373.

<sup>5</sup>M. Stavola, S. J. Pearton, J. Lopata, and W. C. Dautremont-Smith, Appl. Phys. Lett. **50**, 1086 (1987).

<sup>6</sup>M. Stavola, S. J. Pearton, J. Lopata, and W. C. Dautremont-Smith, Phys. Rev. B **37**, 8313 (1988).

<sup>7</sup>C. B. Harris, R. M. Shelby, and P. A. Cornelius, Phys. Rev. Lett. **38**, 1415 (1977).

- <sup>8</sup>M. Budde, G. Lupke, C. Parks Cheney, N. H. Tolk, and L. C. Feldman, *Phys. Rev. Lett.* **85**, 1452 (2000).
- <sup>9</sup>M. Suezawa, N. Fukata, T. Takahashi, M. Saito, and H. Yamada-Kaneta, *Phys. Rev. B* **64**, 085205 (2001).
- <sup>10</sup>B. N. J. Persson and R. Ryberg, *Phys. Rev. B* **40**, 10 273 (1989).
- <sup>11</sup>M. J. Binns, R. C. Newman, S. A. McQuaid, and E. C. Lightowers, *Mater. Sci. Forum* **143–147**, 861 (1994).
- <sup>12</sup>R. E. Pritchard, J. H. Tucker, R. C. Newman, and E. C. Lightowers, *Semicond. Sci. Technol.* **14**, 77 (1999).
- <sup>13</sup>R. E. Pritchard, M. J. Ashwin, J. H. Tucker, R. C. Newman, E. C. Lightowers, M. J. Binns, S. A. McQuaid, and R. Falster, *Phys. Rev. B* **56**, 13 118 (1997).
- <sup>14</sup>V. P. Markevich and M. Suezawa, *J. Appl. Phys.* **83**, 2988 (1998).
- <sup>15</sup>C. G. Van de Walle, *Phys. Rev. B* **49**, 4579 (1994).
- <sup>16</sup>T. Zundel and J. Weber, *Phys. Rev. B* **39**, 13 549 (1989).
- <sup>17</sup>D. E. McCumber and M. D. Sturge, *J. Appl. Phys.* **34**, 1682 (1963).
- <sup>18</sup>R. J. Elliott, W. Hayes, G. D. Jones, H. F. Macdonald, and C. T. Sennett, *Proc. R. Soc. London, Ser. A* **289**, 1 (1965).
- <sup>19</sup>Z. Y. Zhang and David C. Langreth, *Phys. Rev. Lett.* **59**, 2211 (1987).
- <sup>20</sup>Th. Wichert, H. Skudlik, M. Deicher, G. Gruebel, R. Keller, E. Recknagel, and L. Song, *Phys. Rev. Lett.* **59**, 2087 (1987).
- <sup>21</sup>Th. Wichert, H. Skudlik, H.-D. Carstanjen, T. Enders, M. Deicher, G. Gruebel, R. Keller, L. Song, and M. Stutzmann, in *Defects in Electronic Materials*, edited by M. Stavola, S. J. Pearton, and G. Davies, *Mater. Res. Soc. Symp. Proc. No. 104* (Materials Research Society, Pittsburgh, 1988), p. 265.